

Current-voltage Characteristics of Molecular Conductors: Two versus Three Terminal

Prashant Damle, Titash Rakshit, Magnus Paulsson and Supriyo Datta

School of Electrical and Computer Engineering

Purdue University

West Lafayette, IN 47907

Abstract— This paper presents a computational study of the feasibility of a molecular transistor. We address the question of whether a “rigid molecule” (one which does not deform in an external field) used as the conducting channel in a standard three-terminal MOSFET configuration can offer any performance advantage relative to a standard silicon MOSFET. Quantum transport is treated using the Non-Equilibrium Green’s Function (NEGF) formalism. A self-consistent solution of coupled quantum transport and Poisson’s equations shows that the presence of a gate terminal induces asymmetry with respect to the drain voltage polarity in the (otherwise symmetric) two terminal current-voltage characteristic. We show that just as in a conventional MOSFET, the gate oxide thickness needs to be much smaller than the channel length (length of the molecule) for the gate control to be effective. Furthermore, we show that a rigid molecule with metallic source and drain contacts has a temperature independent subthreshold slope much larger than 60 mV/decade , because the metal-induced gap states in the channel prevent it from turning off abruptly. However, this disadvantage can be overcome by using semiconductor contacts.

Keywords— Molecular electronics, MOSFETs, electrostatic analysis, quantum transport, Non-equilibrium Green’s function (NEGF) formalism.

I. INTRODUCTION

MOLECULES are promising candidates as future electronic devices because of their small size, chemical tunability and self-assembly features. Several experimental molecular devices have recently been demonstrated (for a review of the experimental work see [1]). These include two terminal devices where the conductance of a molecule coupled to two contacts shows interesting features such as a conductance gap [2], asymmetry [3] and switching [4]. Then there are three terminal molecular devices like the self-assembled monolayer field effect transistor (SAMFET) [5] where the two terminal current is modulated by using a third (gate) terminal to achieve MOSFET-like behavior.

Molecular devices where a third terminal produces a negative differential resistance [6], or suppresses the two terminal current [7] have been theoretically studied, but most of the work on modeling the current-voltage (IV) characteristics of molecular conductors has focused on two-

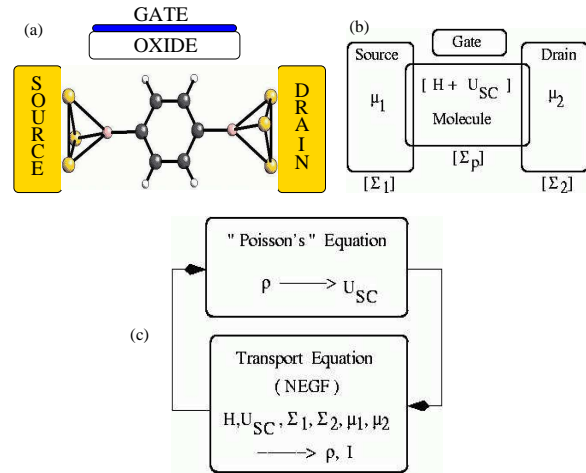


Fig. 1

(A) SCHEMATIC OF A MOLECULE COUPLED TO GOLD SOURCE AND DRAIN CONTACTS. A THIRD (GATE) TERMINAL MAY BE USED TO MODULATE THE CONDUCTANCE OF THE MOLECULE. THE MOLECULE TO GATE COUPLING IS PURELY CAPACITATIVE. (B) THE MOLECULE IS DESCRIBED BY A HAMILTONIAN H AND A SELF-CONSISTENT POTENTIAL U_{SC} . THE EFFECT OF THE LARGE CONTACTS IS DESCRIBED USING SELF-ENERGY MATRICES $\Sigma_{1,2}$. SCATTERING PROCESSES MAY BE DESCRIBED USING ANOTHER SELF-ENERGY MATRIX Σ_p . THE SOURCE AND DRAIN CONTACTS ARE IDENTIFIED BY THEIR RESPECTIVE FERMI LEVELS μ_1 AND μ_2 . GIVEN H , U_{SC} , $\Sigma_{1,2,p}$ AND $\mu_{1,2}$ THE NON-EQUILIBRIUM GREEN’S FUNCTION (NEGF) FORMALISM HAS CLEAR PRESCRIPTIONS TO OBTAIN THE DENSITY MATRIX FROM WHICH THE ELECTRON DENSITY AND CURRENT MAY BE CALCULATED. AT EQUILIBRIUM (ZERO DRAIN BIAS) $\mu_1 = \mu_2 = E_f$, WHERE E_f IS THE COMMON EQUILIBRIUM FERMI LEVEL OF THE CONTACT-MOLECULE-CONTACT SYSTEM. WHEN A DRAIN BIAS V_{DS} IS APPLIED THE SOURCE AND DRAIN FERMI LEVELS SEPARATE BY AN AMOUNT EQUAL TO qV_{DS} (q : ELECTRONIC CHARGE) AND A CURRENT FLOWS. THIS NON-EQUILIBRIUM SITUATION MAY BE MODELED BY SELF-CONSISTENTLY SOLVING THE COUPLED NEGF-POISSON’S EQUATIONS AS SHOWN IN (C). THE WORD “POISSON’S” IS IN QUOTES AS A REMINDER THAT MORE SOPHISTICATED THEORIES LIKE THE HARTREE-FOCK OR THE DENSITY FUNCTIONAL THEORY MAY BE USED TO OBTAIN U_{SC} .

Corresponding author: Supriyo Datta

Telephone: (765) 494 3511

Fax: (765) 494 2706

email: datta@purdue.edu

This work has been submitted to the IEEE for possible publication. Copyright may be transferred without notice, after which this version may no longer be accessible.

terminal devices (see, for example, [8], [9], [10] and references therein). The purpose of this paper is to analyze a three-terminal molecular device assuming that the

molecule behaves essentially like a rigid solid. Unlike solids, molecules are capable of deforming in an external field and it may be possible to take advantage of such conformational effects to design transistors with superior characteristics. However, in this paper we do not consider this possibility and simply address the question of whether a “rigid molecule” used as the conducting channel in a standard three-terminal MOSFET configuration can offer any performance advantage relative to a standard silicon MOSFET. Specifically we will show that: (1) The current-voltage (I-V) characteristics of molecular conductors are strongly influenced by the electrostatics, just like conventional semiconductors. With good gate control, the IV characteristics will saturate for one polarity of the drain bias and increase monotonically if the polarity is reversed. By contrast two-terminal symmetric molecules typically show symmetric I-V characteristics. (2) The only advantage gained by using a molecular conductor for an FET channel is due to the reduced dielectric constant of the molecular environment. To get good gate control the oxide thickness needs to be less than a tenth of the length of the channel (the molecule), whereas in conventional MOSFETs the gate oxide thickness needs to be about 40 times smaller than the channel length. (3) Relatively poor subthreshold characteristics (a *temperature independent* subthreshold slope much larger than 60 mV/decade) are obtained even with good gate control, if metallic contacts (like gold) are used, because the metal-induced gap states in the channel preclude it from turning off abruptly. Preliminary results with a molecule coupled to doped silicon source and drain contacts, however, show a temperature dependent subthreshold slope ($\sim k_B T/q$). We believe this is due to the band-limited nature of the silicon contacts, and we are currently investigating this effect. Overall this study suggests that the superior saturation and subthreshold characteristics reported by Schön et al. [5] can only arise from novel physics beyond that included in our model. Further work on molecular transistors should try to capitalize on the additional degrees of freedom afforded by the “soft” nature of molecular conductors - a feature that is not included in this study.

Section II contains a brief description of the theoretical formulation and the simulation procedure. Section III presents the simulation results along with an explanation of the underlying physics. Section IV summarizes this paper.

II. THEORY

A schematic figure of a molecule coupled to gold contacts (source and drain) is shown in Fig. 1a. As an example we use the Phenyl Dithiol (PDT) molecule which consists of a phenyl ring with thiol (-SH) end groups. A gate terminal may be used to modulate the conductance of the molecule. The coupling between the gate and the molecule is purely capacitative - there is no gate current. We use a simple semi-empirical Hamiltonian H to describe the molecule (Fig. 1b). The effect of the source and drain contacts is taken into account using self-energy functions Σ_1 and Σ_2 [11]. Scattering processes may be described

using another self-energy matrix Σ_p . However, in this paper we focus on coherent or ballistic transport ($\Sigma_p = 0$). The source and drain contacts are identified with their respective Fermi levels μ_1 and μ_2 . Our simulation consists of iteratively solving a set of coupled equations (Fig. 1c) - the Non-Equilibrium Green’s Function (NEGF) formalism [11], [12] equations for the density matrix ρ and the Poisson’s equation for the self-consistent potential U_{SC} . Given H , U_{SC} , Σ_1 , Σ_2 , μ_1 and μ_2 the NEGF formalism has clear prescriptions to obtain the density matrix ρ from which the electron density and the current may be calculated. Once the electron density is calculated we solve the Poisson’s equation to obtain the self-consistent potential U_{SC} . The solution procedure thus consists of two iterative steps:

- **Step 1:** calculate ρ given U_{SC} using NEGF
- **Step 2:** calculate U_{SC} given ρ using Poisson’s equation

The above two steps are repeated till neither U_{SC} nor ρ changes from iteration to iteration. It is worth noting that the self-consistent potential obtained by solving Poisson’s equation (Eq. 11) may be augmented by an appropriate exchange-correlation potential that accounts for many electron effects using schemes like Hartree-Fock (HF) or Density Functional Theory (DFT) [13]. In this paper we do not consider the exchange-correlation effects.

A. Step 1: To obtain ρ from U_{SC}

The central issue in non-equilibrium statistical mechanics is to determine the density matrix ρ ; once it is known, all quantities of interest (electron density, current etc.) can be calculated. A good introductory discussion of the concept of density matrix may be found in [12]. To obtain the density matrix ρ from the self-consistent potential U_{SC} using the NEGF formalism, we need to know the Hamiltonian H , the contact self-energy matrices $\Sigma_{1,2}$ and the contact Fermi levels $\mu_{1,2}$. In this section we describe how we obtain these quantities, and then present a brief outline of the NEGF equations.

Hamiltonian: We use a simple basis consisting of one p_z (or π) orbital on each carbon and sulfur atom. It is well known that the PDT molecule has π conjugation - a cloud of π electrons above and below the plane of the molecule that dictate the transport properties of the molecule [14]. The C-C coupling is 2.5 eV which is widely used to describe carbon nanotubes [15]. The S-C coupling of 1.5 eV is empirically determined to obtain a good fit to the ab initio energy levels obtained using the commercially available quantum chemistry software Gaussian '98 [16]. The comparison to ab initio calculation (Fig. 2) shows that our simple π model describes the PDT molecule fairly well.

Self-energy: Self-energy formally arises out of partitioning the molecule-contact system into a molecular subsystem and a contact subsystem. The contact self-energy Σ is calculated knowing the contact surface Green’s function g and the coupling between the molecule and contact τ . For a molecule coupled to two contacts (source and drain) the molecular Green’s function at an energy E is then written as [11] (I : identity matrix, H : molecular Hamiltonian, U_{SC} : self-consistent potential):

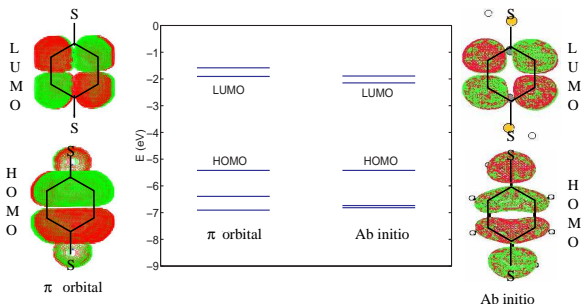


Fig. 2

COMPARISON OF THE SIMPLE π ORBITAL BASED MODEL WITH AN AB INITIO MODEL (DFT WITH ATOMIC ORBITAL BASIS SET) FOR THE PDT MOLECULE. THE ENERGY LEVELS CAN BE DIVIDED IN TWO SETS: OCCUPIED LEVELS (ANALOGOUS TO THE VALENCE BAND) AND UNOCCUPIED LEVELS (ANALOGOUS TO THE CONDUCTION BAND). THE ENERGY GAP (ANALOGOUS TO THE BANDGAP) IS THE ENERGY DIFFERENCE BETWEEN THE HIGHEST OCCUPIED MOLECULAR ORBITAL (HOMO) LEVEL (ANALOGOUS TO THE TOP OF THE VALENCE BAND) AND THE LOWEST UNOCCUPIED MOLECULAR ORBITAL (LUMO) LEVEL (ANALOGOUS TO THE BOTTOM OF THE CONDUCTION BAND). THE SIMPLE π MODEL AGREES VERY WELL WITH THE AB INITIO CALCULATION IN BOTH THE ENERGY GAP (MIDDLE) AND HOMO AND LUMO WAVEFUNCTIONS (LEFT AND RIGHT). THE ENERGY LEVELS OBTAINED FROM THE SIMPLE MODEL WERE EQUALLY SHIFTED IN ENERGY SO AS TO MAKE THE HOMO LEVEL COINCIDE WITH THE AB INITIO HOMO LEVEL.

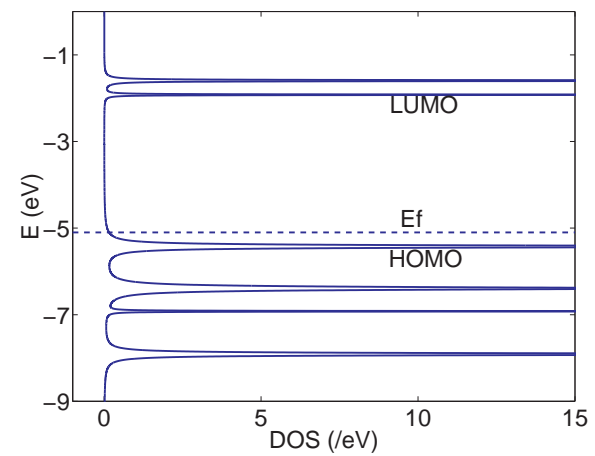


Fig. 3

THE DISCRETE LEVELS OF AN ISOLATED MOLECULE BROADEN INTO A CONTINUOUS DENSITY OF STATES (DOS) UPON COUPLING TO CONTACTS. THE GOLD FCC (111) CONTACTS ARE MODELED USING A BASIS OF ONE 's' TYPE ORBITAL ON EACH GOLD ATOM. THE LUMO WAVEFUNCTION IS LOCALIZED ON THE PHENYL RING (Fig. 2) AND GIVES A SHARP PEAK IN THE DOS. THE HOMO IS DELOCALIZED AND GIVES A COMPARATIVELY BROADENED PEAK IN THE DOS. THE EQUILIBRIUM FERMI ENERGY E_f (~ -5.1 eV FOR BULK GOLD) LIES JUST ABOVE THE HOMO LEVEL.

known as the broadening function:

$$\Gamma_{1,2} = i(\Sigma_{1,2} - \Sigma_{1,2}^\dagger) \quad (3)$$

is related to the lifetime of an electron in a molecular eigenstate. Thus upon coupling to contacts, the molecular density of states (Fig. 3) looks like a set of broadened peaks.

Where is the Fermi energy?: When a molecule is coupled to contacts there is some charge transfer between the molecule and the contacts, and the contact-molecule-contact system attains equilibrium with one Fermi level E_f . A good question to ask is where E_f lies relative to the molecular energy levels. The answer is not clear yet, the position of E_f seems to depend on what contact model one uses. A jellium model [9] for the contacts predicts that E_f is closer to the LUMO level for PDT whereas an extended Hückel theory based model [20] predicts that E_f is closer to the HOMO level (see Fig. 2 and the related caption for a description of HOMO and LUMO levels). Our ab initio model [10] seems to suggest that for gold contacts, E_f (~ -5.1 eV) lies a few hundred millivolts above the PDT HOMO. In this paper we will use $E_f = -5.1$ eV and set the molecular HOMO level (obtained from the π model) equal to the ab initio HOMO level (~ -5.4 eV) (see Figs. 2, 3). Once the location of the equilibrium Fermi energy E_f is known, we can obtain the source and drain Fermi levels μ_1 and μ_2 under non-equilibrium conditions (non-zero V_{DS}): $\mu_1 = E_f$ and $\mu_2 = E_f - qV_{DS}$.

NEGF equations: Given H , $\Sigma_{1,2}$, contact Fermi energies $\mu_{1,2}$ and the self-consistent potential U_{SC} , NEGF has clear prescriptions [11] to obtain the density matrix ρ . The den-

$G = [EI - H - U_{SC} - \Sigma_1 - \Sigma_2]^{-1} \quad (1)$

where the contact self-energy matrices are

$$\Sigma_{1,2} = \tau_{1,2} g_{1,2} \tau_{1,2}^\dagger \quad (2)$$

We model the gold FCC (111) contacts using one s -type orbital on each gold atom. The coupling matrix element between neighboring s orbitals is taken equal to -4.3 eV - this gives correct surface DOS of 0.07 /eV - atom for the gold (111) surface [17]. The site energy for each s orbital is assumed to be -8.74 eV in order to get the correct gold Fermi level of ~ -5.1 eV. The surface Green's function g is calculated using a recursive technique explained in detail in [18]. The contact-molecule coupling τ is determined by the geometry of the contact-molecule bond. It is well known [19] that when a thiol-terminated molecule like Phenyl Dithiol is brought close to a gold substrate, the Hydrogen in the thiol (-SH) group desorbs and the sulfur bonds with three gold atoms arranged in an equilateral triangle. For a good contact extended Hückel theory predicts a coupling matrix element of about 2 eV between the sulfur p_z orbital and the three gold s orbitals. However to simulate the bad contacts typically observed in experiments [2], [9] we reduce the coupling by a factor of five (this factor is also treated as a parameter, and our results do not change qualitatively for a range of values of this parameter).

Unlike the Hamiltonian, the self-energy matrices are non-Hermitian. The anti-Hermitian part of the self-energy, also

sity matrix can be expressed as an energy integral over the correlation function $-iG^<(E)$, which can be viewed as an energy-resolved density matrix:

$$\rho = \int dE [-iG^<(E)/2\pi] \quad (4)$$

The correlation function is obtained from the Green's function G (eq. 1) and the broadening functions $\Gamma_{1,2}$ (eq. 3):

$$-iG^< = G (f_1 \Gamma_1 + f_2 \Gamma_2) G^\dagger \quad (5)$$

where $f_{1,2}(E)$ are the Fermi functions with electrochemical potentials $\mu_{1,2}$:

$$f_{1,2}(E) = \left(1 + \exp \left[\frac{E - \mu_{1,2}}{k_B T} \right] \right)^{-1} \quad (6)$$

The density matrix so obtained can be used to calculate the electron density $n(\vec{r})$ in real space using the eigenvectors of the Hamiltonian $\Psi_\alpha(\vec{r})$ expressed in real space:

$$n(\vec{r}) = \sum_{\alpha, \beta} \Psi_\alpha(\vec{r}) \Psi_\beta^*(\vec{r}) \rho_{\alpha \beta} \quad (7)$$

The total number of electrons N may be obtained from the density matrix as:

$$N = \text{trace}(\rho) \quad (8)$$

The density matrix may also be used to obtain the terminal current [11]. For coherent transport, we can simplify the calculation of the current by using the transmission formalism where the transmission function [11]:

$$T(E) = \text{trace} [\Gamma_1 G \Gamma_2 G^\dagger] \quad (9)$$

is used to calculate the terminal current

$$I = (2q/h) \int_{-\infty}^{\infty} dE T(E) (f_1(E) - f_2(E)) \quad (10)$$

B. Step 2: To obtain U_{SC} from ρ

The Poisson's equation relates the real space potential distribution $U(\vec{r})$ in a system to the charge density $n(\vec{r})$. We assume a nominal charge density $n_0(\vec{r})$ obtained by solving the NEGF equations with $U(\vec{r}) = 0$ (at $V_{GS} = V_{DS} = 0$). The Poisson's equation is then solved for the change in the charge density $(n - n_0)$ from the nominal value n_0 ¹:

$$\vec{\nabla} \cdot (\epsilon \vec{\nabla} U(\vec{r})) = -q^2 (n(\vec{r}) - n_0(\vec{r})) \quad (11)$$

The correct procedure to obtain the real space charge density from the p_z orbital space density matrix ρ is to make use of Eq. 7. However, we simplify the calculation of $n(\vec{r})$ by observing that a carbon or sulfur p_z orbital has a spread of about five to six Bohr radii (1 Bohr radius $a_B = 0.529 \text{ \AA}$). So for each atomic site α we distribute a

¹ The potential distribution corresponding to the nominal charge density (when no drain or gate bias is applied) is included in the calculation of the molecular Hamiltonian [8].

charge equal to $\rho_{\alpha \alpha}$ equally in a cube with side $\sim 10a_B$ centered at site α . This simplification saves a lot of computer time because we do not need to generate the real space wavefunctions $\Psi_\alpha(\vec{r})$ (see Eq. 7).

The Poisson (or Hartree) potential U may be augmented by an appropriate exchange-correlation potential U_{xc} . In this paper, we do not take into account the exchange-correlation effects ($U_{xc} = 0$). We have two schemes to solve the Poisson's equation: (1) simple Capacitance Model and (2) numerical solution over a 2D grid in real space.

Capacitance Model: We use a simplified picture of the molecule as a quantum dot with some nominal *total* charge N_0 (at $V_{GS} = V_{DS} = 0$) and some average potential U arising because of the *change* $N - N_0$ in this nominal charge due to the applied bias. Thus U , N_0 and N are numbers and not matrices. The total charge N can be calculated from the NEGF density matrix using Eq. 8. U is the solution to the Poisson's equation, and may be written as the sum of two terms: (1) A Laplace (or homogeneous) solution U_L with zero charge on the molecule but with applied bias and (2) A particular (or inhomogeneous) solution U_P with zero bias but with charge present on the molecule. Thus $U = U_L + U_P$. U_L is easily written down in terms of the capacitative couplings C_{MS} , C_{MD} and C_{MG} of the molecule (Fig. 4) with the source, drain and gate respectively:

$$U_L = \beta(-qV_{GS}) + \frac{(1 - \beta)}{2}(-qV_{DS}) \quad (12)$$

where

$$\beta = \frac{C_{MG}}{C_{MS} + C_{MD} + C_{MG}} \quad (13)$$

is a parameter ($0 < \beta < 1$) and is a measure of how good the gate control is. Gate control is ideal when C_{MG} is very large as compared to C_{MS} and C_{MD} ². In this case, $\beta = 1$ and the Laplace solution $U_L = -qV_{GS}$ is essentially tied to the gate. An estimate of gate control may be obtained from the numerical grid solution explained below by plotting β as a function of gate oxide thickness t_{ox} (Fig. 8).

The particular solution U_P may be written in terms of a charging energy U_0 as:

$$U_P = U_0(N - N_0) \quad (14)$$

The charging energy is treated as a parameter, and may be estimated as follows. The capacitance of a sphere of radius R is $4\pi\epsilon R$. If we distribute a charge of one electron on this sphere, the potential of the sphere is $q/4\pi\epsilon R$. For $R = 1 \text{ nm}$ the value of this potential is about 1.4 eV. Thus we use a charging energy $U_0 \sim 1 \text{ eV}$. U_0 is the charging energy per electron per molecule and may also be estimated from the numerical grid solution by finding the average potential in the region occupied by the molecule and carrying

² We have assumed that $C_{MS} = C_{MD}$ in eq. 12, which is reasonable because the center of the molecule is equidistant from the source and drain contacts in our model (see Fig. 1). In general, if the source (drain) is closer to the molecule, then C_{MS} (C_{MD}) will be bigger [8]. With $C_{MS} = C_{MD}$, the molecular Laplace potential is $V_{DS}/2$ in the absence of a gate ($\beta = 0$), as is evident from eq. 12 (also see Fig. 6c,d and the related caption).

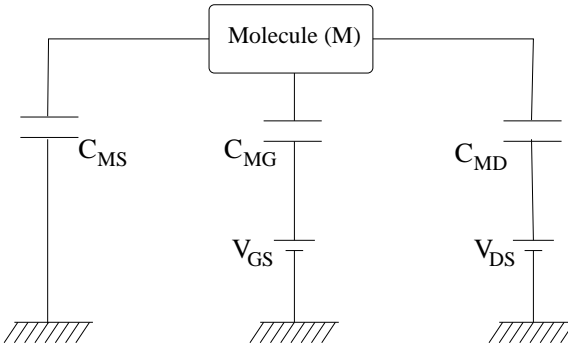


Fig. 4

EQUIVALENT CIRCUIT MODEL USED TO OBTAIN THE HOMOGENEOUS (OR ZERO CHARGE) SOLUTION TO THE POISSON'S EQUATION. THE MOLECULAR POTENTIAL IS CONTROLLED BY THE GATE IF THE CAPACITATIVE COUPLING C_{MG} BETWEEN THE MOLECULE AND THE GATE IS MUCH GREATER THAN THE CAPACITATIVE COUPLINGS C_{MS} AND C_{MD} BETWEEN THE MOLECULE AND THE SOURCE AND DRAIN RESPECTIVELY (SEE Eqs. 12, 13 AND RELATED DISCUSSION).

one electronic charge distributed equally. This numerical procedure also yields $U_0 \sim 1 \text{ eV}$ and is used to estimate the charging energy while comparing the capacitance model with the numerical grid solution (see Fig. 9 and the related caption).

With the simple capacitance model just described, the Poisson's solution U is just a number. The self-consistent potential that adds to the p_z Hamiltonian (see Eq. 1) is then calculated as $U_{SC} = UI$, where I is the identity matrix of the same size as that of the Hamiltonian.

Numerical solution: We use a 2D real space grid to solve the discretized Poisson's equation for the geometry shown in Fig. 1a. The applied gate, source and drain voltages provide the boundary conditions. We use a dielectric constant of 3.9 for silicon dioxide and 2 for the self-assembled monolayer (SAM) [21]. The solution to Poisson's equation yields the real space potential distribution. However, the self-consistent potential U_{SC} that needs to be added to the Hamiltonian (Eq. 1) is in the p_z orbital space. We assume that U_{SC} is a diagonal matrix with each diagonal entry as the value of the real space solution U at the appropriate atomic position. For example, the diagonal entry in U_{SC} corresponding to the sulfur based p_z orbital would be equal to $U(\vec{r}_S)$ where \vec{r}_S is the position vector of the sulfur atom.

III. RESULTS

The self-consistent procedure (Fig. 1c) is done with the two types of Poisson solutions discussed above. The simple capacitance model is fast while the 2D numerical solution is slow but more accurate. The capacitance model has two parameters, namely β which is a measure of the gate control, and U_0 which is the charging energy. These parameters can be extracted using the 2D numerical solution. We will first present results with the capacitance model by assuming ideal gate control, or $\beta = 1$. This ideal case is useful to explain the current saturation mechanism. We will then

compare the results obtained from the capacitance model with those obtained from the numerical solution, and show that the two match reasonably well.

A. Ideal gate control, on state

Fig. 5 shows the molecular IV characteristic obtained by self-consistently solving the coupled NEGF - capacitance model Poisson's equations. We contrast the IV for ideal gate control ($\beta = 1$, Fig. 5a,b) with that for no gate control ($\beta = 0$, Fig. 5c,d). For each case, we have shown the IV for positive as well as negative drain voltage. We observe the following:

- With ideal gate control the IV is asymmetric with respect to the drain bias. For positive drain bias, we see very little gate modulation of the current. For negative drain bias we see current saturation and good gate modulation - the IV looks like that of a MOSFET.
- With no gate control the IV is symmetric with respect to the drain bias. There is no gate modulation.

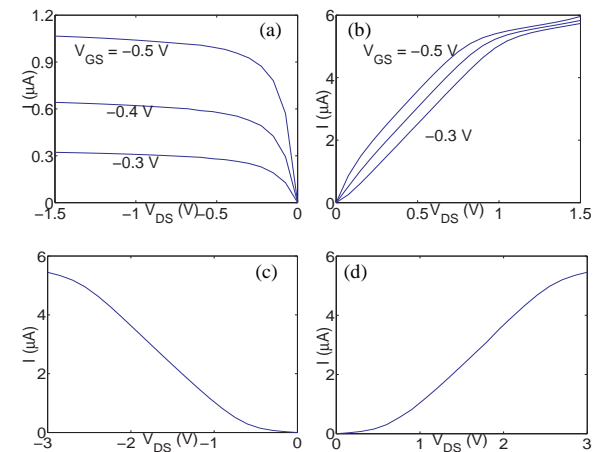


Fig. 5

THREE TERMINAL MOLECULAR DRAIN CURRENT VS. DRAIN TO SOURCE VOLTAGE CHARACTERISTIC WITH (A) IDEAL GATE CONTROL ($\beta = 1$), (B) IDEAL GATE CONTROL, POSITIVE DRAIN BIAS, (C) NO GATE CONTROL ($\beta = 0$), NEGATIVE DRAIN BIAS AND (D) NO GATE CONTROL, POSITIVE DRAIN BIAS. WITH IDEAL GATE CONTROL THE IV IS ASYMMETRIC WITH RESPECT TO DRAIN BIAS. GOOD SATURATION AND GATE MODULATION IS SEEN FOR NEGATIVE DRAIN BIAS BUT NOT FOR POSITIVE DRAIN BIAS. WITH NO GATE CONTROL THE IV IS SYMMETRIC WITH RESPECT TO DRAIN BIAS. FOR AN EXPLANATION OF THE UNDERLYING MECHANISM FOR EACH OF THESE IV CURVES, SEE FIG. 6.

These features of the IV characteristic may be understood as follows (Fig. 6). Let us first consider the ideal gate case. Since the gate is held at a fixed potential *with respect to the source*, the molecular DOS does not shift relative to the source Fermi level μ_1 as the drain bias is changed³. For negative drain bias (Fig. 6a), the drain

³ This is true as long as the charging energy $U_0 \sim 1 \text{ eV}$, which is typically the case. For high charging energies the particular solution U_P can dominate the Laplace solution U_L (see eqs. 12,14 and related discussion), thereby reducing gate control.

Fermi level μ_2 moves up (towards the LUMO) with respect to the molecular DOS. Since the drain current depends on the DOS lying between the source and drain Fermi levels, the current saturates for increasing negative drain bias because the tail of the DOS dies out as the drain Fermi level moves towards the LUMO. If the gate bias is now made more negative, the molecular DOS shifts up towards the source Fermi level, thereby bringing in more DOS in the energy range between μ_1 and μ_2 (referred to as the μ_1 - μ_2 window from hereon), and the current increases. Thus we get current saturation and gate modulation.

For positive drain bias (Fig. 6b), μ_2 moves down (towards the HOMO) with respect to the molecular DOS. The current increase with positive drain bias because more and more DOS is coming inside the μ_1 - μ_2 window as μ_2 moves towards the HOMO peak. Once μ_2 crosses the HOMO peak, the current levels off. This is the resonant tunneling mechanism. If the gate bias is now made more negative, no appreciable change is made in the DOS inside the μ_1 - μ_2 window, and the maximum current remains almost independent of the gate bias.

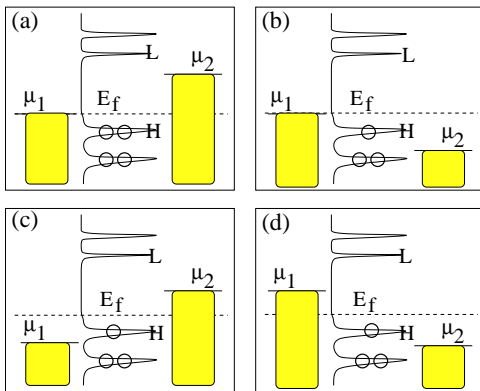


Fig. 6

GATE INDUCED CURRENT SATURATION MECHANISM: ASSUMING THAT THE GATE IS VERY CLOSE TO THE MOLECULE (IDEAL GATE CONTROL, $\beta = 1$), THE GATE HOLDS THE MOLECULAR DOS FIXED RELATIVE TO THE SOURCE FERMI LEVEL μ_1 BECAUSE THE GATE IS HELD AT A FIXED POTENTIAL WITH RESPECT TO THE SOURCE. WHEN A NEGATIVE DRAIN BIAS IS APPLIED (TOP LEFT), THE DRAIN FERMI LEVEL μ_2 MOVES UP RELATIVE TO THE MOLECULAR DOS. SINCE THE DOS DIES OUT IN THE GAP, FOR SUFFICIENTLY HIGH DRAIN BIAS, NO MORE DOS COMES IN THE μ_1 - μ_2 WINDOW AND THE CURRENT SATURATES. WHEN A POSITIVE DRAIN BIAS IS APPLIED (TOP RIGHT), μ_2 MOVES DOWN RELATIVE TO DOS AND EVENTUALLY CROSSES THE HOMO. THE IV IS thus ASYMMETRIC. IF THE GATE IS FAR AWAY (NO GATE CONTROL, $\beta = 0$), THE DOS LIES ROUGHLY HALFWAY BETWEEN THE SOURCE AND DRAIN FERMI LEVELS. IN THIS CASE, FOR NEGATIVE DRAIN BIAS (BOTTOM LEFT), μ_1 CROSSES HOMO WHILE FOR POSITIVE DRAIN BIAS (BOTTOM RIGHT) μ_2 CROSSES HOMO. NO GATE MODULATION IS SEEN AS EXPECTED, AND THE CURRENT IS SYMMETRIC WITH RESPECT TO DRAIN BIAS.

Now let us contrast this with the case where no gate is present. In this case, due to the applied drain bias V_{DS} , the molecular DOS floats up by roughly $-qV_{DS}/2$ with respect

to the source Fermi level. For either negative (Fig. 6c) or positive (Fig. 6d) drain bias, the current flow mechanism is resonant tunneling. Since the equilibrium Fermi energy lies closer to the HOMO, for negative drain bias μ_1 crosses HOMO while for positive drain bias μ_2 crosses HOMO [8], [22]. No gate modulation is seen as expected, and the IV is symmetric with respect to V_{DS} .

B. Ideal gate control - off state

Fig. 7 shows the log scale drain current as a function of gate bias at high drain bias. We note that despite assuming ideal gate control, the subthreshold slope of this molecular FET is about 300 mV/decade which is much worse than the ideal room temperature $k_B T/q = 60 \text{ mV/decade}$ that a good MOSFET can come close to achieving. It is also worth noting here that our simulation is done at low temperature - the subthreshold slope of the molecular FET is *temperature independent* and only depends on the molecular DOS as explained below.

The poor subthreshold slope may be understood as follows. As the gate voltage is made more positive, the molecular DOS shifts down with respect to the μ_1 - μ_2 window. The HOMO peak thus moves away from the μ_1 - μ_2 window, and fewer states are available to carry the current. The rate at which the current decreases with increasing positive gate bias thus depends on the rate at which the tail of the DOS in the HOMO-LUMO gap dies away with increasing energy (Fig. 3). Typically we find that the tail of the DOS dies away at the rate of several hundred milli electron-volts of energy per decade, and this slow fall in the DOS determines the subthreshold slope. The slow fall in the molecular DOS may be attributed to the metal-induced gap (MIG) states - the gold source and drain contacts have a sizeable DOS near the Fermi energy, and are separated only by a few angstroms⁴. Since the molecule is assumed to be rigid, the molecular DOS has no temperature dependence and hence neither does the subthreshold slope.

Thus the molecular FET is a very poor switching device even with ideal gate control. This of course assumes that the molecule is rigid and the gate bias just shifts the molecular DOS without drastically changing the shape of the DOS. Gate induced conformational changes in the molecular geometry may well change the shape of the DOS, but this effect is not included in our model.

C. Estimate of Gate Control

The 2D numerical Poisson's solution may be used to estimate the gate control as follows. From Eq. 12 we see that

⁴ For ballistic silicon MOSFETs, due to the band-limited nature of the doped silicon source/drain contacts, the MIG DOS is negligible. The subthreshold slope at a finite temperature is thus determined by the rate at which the difference in the source and drain *Fermi function tails* falls as a function of energy. This rate depends on the temperature, and the subthreshold slope is thus proportional to $k_B T/q$ ($\approx 60 \text{ mV}$ at room temperature) for ballistic Si MOSFETs [23]. Preliminary results for a molecular FET with doped silicon source and drain contacts do show a subthreshold slope proportional to $k_B T/q$; we are currently investigating this effect.

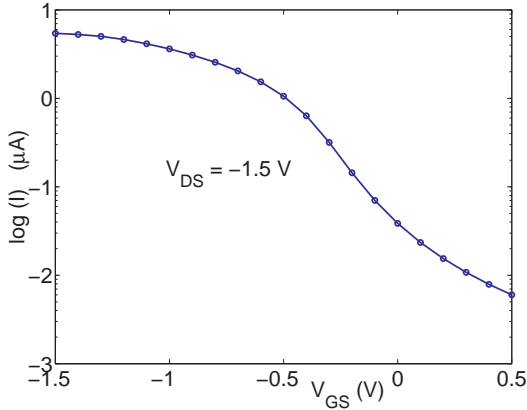


Fig. 7

SUBTHRESHOLD IV CHARACTERISTIC ASSUMING IDEAL GATE CONTROL. THE SUBTHRESHOLD SLOPE IS $\sim 300 \text{ mV/decade}$ EVEN WITH AN IDEAL GATE. THIS IS BECAUSE THE DOS IN THE HOMO-LUMO GAP DIES OUT VERY SLOWLY AS A FUNCTION OF ENERGY. THIS SLOW FALL OF THE DOS MAY BE ATTRIBUTED TO THE GOLD METAL-INDUCED GAP STATES. THUS A MOLECULAR FET WITH A RIGID MOLECULE COUPLED TO GOLD SOURCE/DRAIN CONTACTS IS A VERY POOR SWITCH. GATE INDUCED CONFORMATIONAL CHANGES IN THE MOLECULAR GEOMETRY MAY CHANGE THE SHAPE OF THE DOS IN ADDITION TO SHIFTING IT, THUS POSSIBLY PRODUCING A FAST SWITCH-OFF. SUCH CONFORMATIONAL CHANGE EFFECTS ARE NOT INCLUDED IN OUR MODEL.

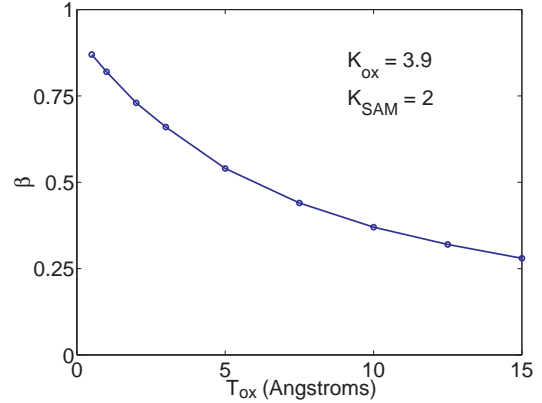


Fig. 8

ESTIMATE OF GATE CONTROL USING 2D NUMERICAL LAPLACE SOLUTION. β (WHICH IS A MEASURE OF GATE CONTROL, SEE Eqs. 12, 13) IS PLOTTED AS A FUNCTION OF THE GATE OXIDE THICKNESS T_{ox} . THE LENGTH OF PDT MOLECULE (EQUAL TO THE CHANNEL LENGTH OF THE MOLECULAR FET) IS ABOUT 1 nm. THUS IN ORDER TO GET GOOD GATE CONTROL ($\beta > 0.8$) THE GATE OXIDE THICKNESS HAS TO BE ABOUT ONE TENTH OF THE CHANNEL LENGTH, OR ABOUT 1 Å! WE HAVE USED 3.9 AND 2 AS THE DIELECTRIC CONSTANTS FOR SILICON DIOXIDE AND THE SELF-ASSEMBLED MONOLAYER (SAM) RESPECTIVELY. WITH A HIGH DIELECTRIC CONSTANT GATE INSULATOR MATERIAL (E.G. WATER HAS A DIELECTRIC CONSTANT OF ABOUT 80) IT WOULD BE POSSIBLE TO ACHIEVE GOOD GATE CONTROL WITH OXIDE THICKNESSES OF THE ORDER OF 1 nm.

$$\beta = \frac{\partial U_L}{\partial V_{GS}} \quad (15)$$

Thus β may be estimated from the numerical solution by slightly changing V_{GS} and calculating how much the Laplace solution changes over the region occupied by the molecule. A plot of β calculated using this method as a function of the gate oxide thickness T_{ox} is shown in Fig. 8.

Knowing that the channel length (length of the PDT molecule) is about 1 nm, It is evident from Fig. 8 that in order to get good gate control ($\beta > 0.8$) the gate oxide thickness (T_{ox}) needs to be about one tenth of the channel length (L_{ch}), or about 1 Å! Thus we need $L_{ch}/T_{ox} \sim 10$ to get a good molecular FET. In a well-designed conventional bulk MOSFET, $L_{ch}/T_{ox} \sim 40$ [24]. This difference between a molecular FET and a conventional FET may be understood by noting that the dielectric constant of the molecular environment (=2) is about 6 times smaller than that of silicon (=11.7) [25].

D. Comparison: Capacitance model vs. Numerical Poisson's solution

Fig. 9 compares the IV characteristic obtained by solving the self-consistent NEGF-Poisson's equations with the numerical Poisson's solution and the capacitance model. The parameters β and U_0 for the capacitance model were extracted from the numerical solution. We see a reasonable agreement between the two solutions despite the simplifications made in the capacitance model (the capacitance

model assumes a flat potential profile in the region occupied by the molecule, which may not be true, especially at high bias). For $t_{ox} = 1.5 \text{ nm}$ (Fig. 9a) there is very little gate modulation and no saturation as expected. In this case $\beta = 0.28$ (Fig. 8) and the IV resembles that shown in Fig. 5c more than the one in Fig. 5a. Also seen in Fig. 9 are the results for $t_{ox} = 1 \text{ Å}$. For this case $\beta = 0.82$ and we observe reasonable saturation and gate control. For realistic oxide thicknesses, however, we expect to observe an IV like the one shown in Fig. 9a as long as we consider the molecule to be rigid and the gate just shifts the molecular DOS.

IV. CONCLUSION

We have presented simulation results for a three terminal molecular device. The NEGF equations for quantum transport are self-consistently solved with the Poisson's equation. We conclude the following:

1. If the molecule is considered to be rigid, with the gate voltage just shifting the molecular levels up or down relative to the source and drain Fermi levels, the gate oxide thickness needs to be about a tenth of the length of the molecule to get good gate control.
2. Given good gate control, the drain current is expected to be asymmetric with respect to the drain voltage polarity. Such asymmetry is also expected for a conventional silicon MOSFET [25].

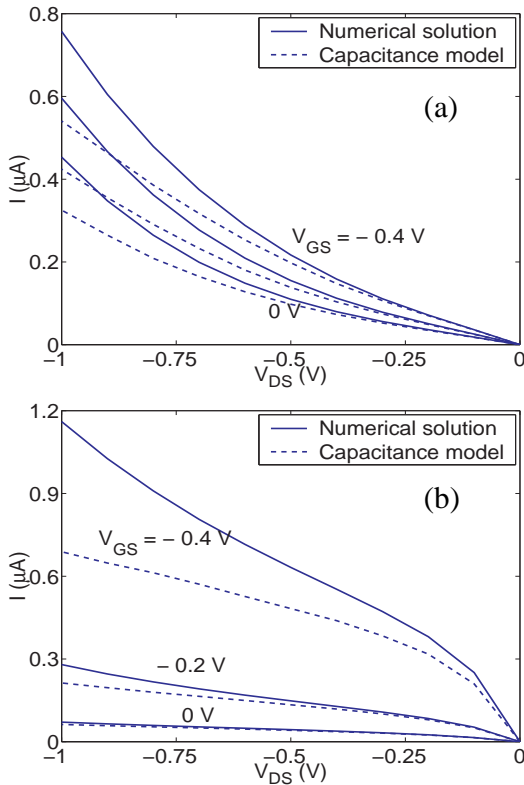


Fig. 9

COMPARISON OF THE NUMERICAL POISSON SOLUTION WITH THE CAPACITANCE MODEL. WE SEE REASONABLE AGREEMENT IN THE TWO SOLUTIONS DESPITE THE SIMPLIFICATIONS MADE IN THE CAPACITANCE MODEL. (A) A REALISTIC CASE WITH $t_{ox} = 1.5 \text{ nm}$ WHICH YIELDS $\beta = 0.28$ AND $U_0 = 1.9 \text{ eV}$. NO CURRENT SATURATION IS SEEN, BUT SOME GATE MODULATION IS PRESENT. (B) AN "ABSURD" CASE WITH $t_{ox} = 1 \text{ \AA}$ WHICH YIELDS $\beta = 0.82$ AND $U_0 = 1 \text{ eV}$ (U_0 IS LESS FOR THIS CASE BECAUSE THE GATE IS CLOSER TO THE MOLECULE; SCREENING EFFECT OF THE GATE ELECTRODE IS LARGER). THE IV FOR THIS CASE LOOKS LIKE THAT FOR A MOSFET. SIMILAR IV MAY BE OBTAINED WITH $t_{ox} = 1 \text{ nm}$, PROVIDED ONE USES A GATE INSULATOR WITH A DIELECTRIC CONSTANT ABOUT TEN TIMES THAT OF SILICON DIOXIDE.

3. Even with ideal gate control, the subthreshold slope of a molecular FET with metallic source/drain contacts is expected to be larger than 60 mV/decade and is independent of temperature. Preliminary results show that a temperature dependent subthreshold slope ($\sim k_B T/q$) can be obtained with silicon source/drain contacts. We are currently investigating this effect.

4. In order to understand the superior transistor action seen in Schön's SAMFET experiment (good gate control with $\sim 1 \text{ nm}$ channel length and $\sim 4 \text{ nm}$ thick gate oxide, symmetric IVs with respect to drain voltage polarity, subthreshold slope less than 60 mV/decade [5], [26]), some novel physics other than that contained in our model needs to be understood.

5. Further work on molecular transistors should try to exploit the additional degrees of freedom afforded by the

"soft" (as opposed to rigid) nature of molecular conductors.

Acknowledgments: We would like to thank J.H. Schön, M. Samanta, A. Ghosh, R. Venugopal and M. Lundstrom for useful discussions. This work was supported by the NSF under grants number 9809520-ECS and 0085516-EEC and by the Semiconductor Technology Focus Center on Materials, Structures and Devices under contract number 1720012625.

REFERENCES

- [1] M.A. Reed, "Molecular-scale electronics," *Proc. IEEE*, vol. 87, pp. 652, 1999.
- [2] M.A. Reed, C. Zhou, C.J. Muller, T.P. Burgin, and J.M. Tour, "Conductance of a molecular junction," *Science*, vol. 278, pp. 252, 1997.
- [3] J. Reichert, R. Ochs, D. Beckmann, H.B. Weber, M. Mayor, and H.v. Löhneysen, "Driving current through single organic molecules," *cond-mat/0106219*.
- [4] J. Chen, M.A. Reed, A.M. Rawlett, and J.M. Tour, "Observation of a large on-off ratio and negative differential resistance in an electronic molecular switch," *Science*, vol. 286, pp. 1550, 1999.
- [5] J.H. Schön, H. Meng, and Z. Bao, "Self-assembled monolayer organic field-effect transistors," *Nature*, vol. 413, pp. 713, 2001.
- [6] M. Di Ventra, S.T. Pantelides, and N.D. Lang, "The benzene molecule as a molecular resonant-tunneling transistor," *Appl. Phys. Lett.*, vol. 76, pp. 3448, 2000.
- [7] E. Emberly and G. Kirczenow, "Multiterminal molecular wire systems: A self-consistent theory and computer simulations of charging and transport," *Phys. Rev. B*, vol. 62, pp. 10451, 2000.
- [8] S. Datta, W. Tian, S. Hong, R. Reifenberger, J. I. Henderson, and C.P. Kubiak, "Current-voltage characteristics of self-assembled monolayers by scanning tunneling microscopy," *Phys. Rev. Lett.*, vol. 79, pp. 2530, 1997.
- [9] M. Di Ventra, S.T. Pantelides, and N.D. Lang, "First-principles calculation of transport properties of a molecular device," *Phys. Rev. Lett.*, vol. 84, pp. 979, 2000.
- [10] P.S. Damle, A.W. Ghosh, and S. Datta, "Unified description of molecular conduction: from molecules to metallic wires," *Phys. Rev. B (Rapid Comm.)*, vol. 64, pp. 201403, 2001.
- [11] S. Datta, *Electronic Transport in Mesoscopic Systems*, Cambridge University Press, 1995.
- [12] S. Datta, "Nanoscale device modeling: the green's function method," *Superlattices and Microstructures*, vol. 28, pp. 253, 2000.
- [13] A. Szabo and N.S. Ostlund, *Modern Quantum Chemistry*, Dover Publications, Inc., Mineola, New York, 1996.
- [14] Magnus Paulsson and Sven Stafström, "Self-consistent-field study of conduction through conjugated molecules," *Phys. Rev. B*, vol. 64, pp. 035416, 2001.
- [15] R. Saito, G. Dresselhaus, and M.S. Dresselhaus, *Physical Properties of Carbon Nanotubes*, Imperial College Press, 1998.
- [16] M. J. Frisch, G. W. Trucks, H. B. Schlegel, G. E. Scuseria, M. A. Robb, J. R. Cheeseman, V. G. Zakrzewski, J. A. Montgomery, Jr., R. E. Stratmann, J. C. Burant, S. Dapprich, J. M. Millam, A. D. Daniels, K. N. Kudin, M. C. Strain, O. Farkas, J. Tomasi, V. Barone, M. Cossi, R. Cammi, B. Mennucci, C. Pomelli, C. Adamo, S. Clifford, J. Ochterski, G. A. Petersson, P. Y. Ayala, Q. Cui, K. Morokuma, D. K. Malick, A. D. Rabuck, K. Raghavachari, J. B. Foresman, J. Ciosowski, J. V. Ortiz, A. G. Baboul, B. B. Stefanov, G. Liu, A. Liashenko, P. Piskorz, I. Komaromi, R. Gomperts, R. L. Martin, D. J. Fox, T. Keith, M. A. Al-Laham, C. Y. Peng, A. Nanayakkara, C. Gonzalez, M. Challacombe, P. M. W. Gill, B. G. Johnson, W. Chen, M. W. Wong, J. L. Andres, M. Head-Gordon, E. S. Replogle and J. A. Pople, Gaussian, Inc., Pittsburgh PA, "Gaussian 98 (revision a.7)," 1998.
- [17] D.A. Papaconstantopoulos, *Handbook of the Band Structure of Elemental Solids*, Plenum Press, New York, 1986.
- [18] M. Samanta, "Electronic conduction through organic molecules," M.S. thesis, Purdue University, 1995.
- [19] N. B. Larsen, H. Biebuyck, E. Delamarche, and B. Michel, "Order in microcontact printed self-assembled monolayers," *J. Am. Chem. Soc.*, vol. 119, pp. 3107, 1997.

- [20] W. Tian, S. Datta, S. Hong, R. Reifenberger, J. I. Henderson, and C.P. Kubiak, "Conductance spectra of molecular wires," *J. Chem. Phys.*, vol. 109, pp. 2874, 1998.
- [21] M.A. Rampi, O.J.A. Schueller, and G.M. Whitesides, "Alkanethiol self-assembled monolayers as the dielectric of capacitors with nanoscale thickness," *Appl. Phys. Lett.*, vol. 72, pp. 1781, 1998.
- [22] F. Zahid, M. Paulsson, and S. Datta, "Electrical conduction through molecules," to appear in forthcoming volume on Advanced Semiconductors and Organic Nano-Techniques, edited by H. Morkoc, Academic Press, 2002.
- [23] Z. Ren, R. Venugopal, S. Datta, M. Lundstrom, D. Jovanovic, and J. Fossum, "The ballistic nanotransistor: a simulation study," *IEDM Tech. Dig.*, p. 715, 2000.
- [24] Y. Taur and T. Ning, *Fundamentals of VLSI Devices*, Cambridge University Press, Cambridge, UK, 1998.
- [25] M. Lundstrom (private communication), 2002 .
- [26] J.H. Schön (private communication), 2002 .